

–Supporting Information–

Elucidating Lithium-Ion and Proton Dynamics in Anti-Perovskite Solid Electrolytes

James A. Dawson,^{1*} Tavleen S. Attari,² Hungru Chen,¹ Steffen P. Emge,³ Karen E.

Johnston^{2*} and M. Saiful Islam^{1*}

¹Department of Chemistry, University of Bath, Bath, BA2 7AY, UK

²Department of Chemistry, Durham University, Durham, DH1 3LE, UK

³Department of Chemistry, University of Cambridge, Cambridge, CB2 1EW, UK

Table of Contents:

Experimental Methods	S2
Figure S1: XRD patterns of Li ₃ OCl	S4
Figure S2: Rietveld refinement of XRD data for cubic phase of Li ₂ OHCl	S5
Table S1: Structural parameters for cubic phase of Li ₂ OHCl obtained from Rietveld data	S5
Figure S3: XRD and SSNMR data for the series Li _{2.75} OH _{0.25} Cl	S6
Figure S4: XRD and SSNMR data for the series Li _{2.25} OH _{0.75} Cl	S7
Figure S5: Variation in ¹ H and ⁷ Li FWHM as a function of composition for Li _{3-x} OH _x Cl	S8
Figure S6: Variation in ⁷ Li FWHM obtained from static VT NMR data	S9
Scheme 1: Pulse sequence used for the acquisition of ⁷ Li PFG-NMR spectra	S10
Figure S7: Variation in I/I_0 with gradient strength for different diffusion times for Li ₂ OHCl at 373 K	S11
Figure S8: Plots of $\ln[I/I_0]$ vs. b for Li ₂ OHCl at 373 K, including fitted data	S12
Table S2: Li diffusion coefficients, D_{Li} , obtained for Li ₂ OHCl at 373 K	S12
Figure S9: Trend in Li diffusion coefficients for Li ₂ OHCl at 373 K as a function of the diffusion time	S13
Figure S10: ¹ H PFG-NMR experiments	S14
Figure S11: XRD pattern for Li ₂ ODCl	S15
Figure S12: Static VT ² H NMR spectra for Li ₂ ODCl	S16
Figure S13: Simulation of ² H MAS NMR data obtained at 33 °C	S16
References	S17

Experimental Methods

NMR Spectroscopy. Typically, a broad background signal is observed in the ^1H MAS NMR spectra of samples with a low concentration of ^1H . Hence, to overcome this, a “depth” pulse sequence is used for background suppression. All ^1H MAS NMR spectra were acquired using a background suppression (DEPTH)¹ experiment with typical $\pi/2$ and π pulse lengths of 4 and 8 μs , respectively. Conventional ^7Li MAS NMR spectra were obtained using a single-pulse experiment with a typical pulse length of 1.5 μs . During the acquisition, proton-decoupling was applied using SPINAL-64,² with a RF field of 32 kHz. The experimentally optimised recycle intervals for ^1H and ^7Li were 60 s. Typical radiofrequency field strengths of 62–166 kHz were employed. Static ^7Li NMR spectra were acquired using a solid echo experiment with a typical pulse length of 1 μs . ^1H and ^7Li T_1 values were measured using a saturation recovery experiment. Static and MAS ^2H NMR spectra were obtained using a solid echo experiment with a typical pulse length of 4 μs , recycle interval of 5 s and RF field of 62.5 kHz.

Verification of the H content of samples in the series $\text{Li}_{3-x}\text{OH}_x\text{Cl}$. A ^1H MAS NMR spectrum was obtained for a pre-weighed sample of adamantane. The spectrum was integrated and the integral was manually set to an arbitrary value of 100. From this, the number of protons present in the sample can be determined as follows:

Adamantane ($\text{C}_{10}\text{H}_{16}$):

Mass = 0.0614 g, $M_r = 136 \text{ g mol}^{-1}$

\therefore no. of moles = $0.0614 \text{ g} \times 136 \text{ g mol}^{-1} = 4.51 \times 10^{-4} \text{ mol}$

No. of adamantane molecules = no. of moles \times Avogadro's constant = $4.51 \times 10^{-4} \text{ mol} \times 6.02 \times 10^{23} \text{ mol}^{-1} = 2.72 \times 10^{20}$

No. of protons in the sample = No. of adamantane molecules \times No. of protons in 1 adamantane molecule = $2.72 \times 10^{20} \times 16 = 4.352 \times 10^{21}$

The integral was manually set to 100. Therefore, an integral of 100 corresponds to 4.352×10^{21} protons. It follows that an integral of 1 corresponds to 4.352×10^{19} protons.

^1H MAS NMR spectra were obtained for each sample in the series $\text{Li}_{3-x}\text{OH}_x\text{Cl}$ ($x = 0.25, 0.5, 0.75$). The H content of $\text{Li}_{2.25}\text{OH}_{0.75}\text{Cl}$ was verified using the method outlined below:

The ^1H MAS NMR spectrum of $\text{Li}_{2.25}\text{OH}_{0.75}\text{Cl}$ was integrated using “the last calibrated scale”. This integrates the spectrum using the scale previously used for the pre-weighed sample of adamantane.

For $\text{Li}_{2.25}\text{OH}_{0.75}\text{Cl}$ an integral of 2.3890 was obtained.

According to the last scale used, an integral of 1 corresponds to 4.352×10^{19} protons. Therefore, an integral of 2.3890 corresponds to 1.04×10^{20} protons.

Mass of sample = 0.1251 g

No. of protons in 1 g of sample = 1.04×10^{20} protons/ 0.1251 g = 8.31×10^{20} protons g⁻¹

If a sample of Li_{3-x}OH_xCl contains 8.31×10^{20} protons, then what is x?

We need to find out how many Li_{3-x}OH_xCl units are present in the sample and how many protons each unit contains.

Mass of sample = 0.1251 g

Mr of Li_{3-x}OH_xCl is 72.27 - 59.4x (Mr of Li_{3-x}OH_xCl = 6.94(3-x) + 16 + 1(x) + 35.45)

∴ no. of moles = mass of sample/ Mr of Li_{3-x}OH_xCl = (0.1251 g/ 72.27 - 59.4x) mol

No. of Li_{3-x}OH_xCl units in the sample = no. of moles × Avogadro's constant = (0.1251 g/ 72.27 - 59.4x) mol × 6.02×10^{23} mol⁻¹ = (7.53×10^{22} / 72.27 - 59.4x)

These Li_{3-x}OH_xCl units contain x no. of protons (8.31×10^{20})

Therefore, (7.53×10^{22} x/ 72.27 - 59.4x) = 8.31×10^{20} protons

Rearrange to find x:

$$(7.53 \times 10^{22} \text{ x} / 72.27 - 59.4\text{x}) = 8.31 \times 10^{20}$$

$$7.53 \times 10^{22} \text{ x} = 8.31 \times 10^{20} (72.27 - 59.4\text{x})$$

$$\text{x} = 0.011 (72.27 - 59.4\text{x})$$

$$\text{x} = 0.0795 - 0.0653\text{x}$$

$$\text{x} + 0.0653\text{x} = 0.0795$$

$$\text{x} = 0.746$$

$$\text{x} = 0.75$$

This indicates that for this sample of Li_{3-x}OH_xCl, x = 0.75.

The same method was used for each of the remaining samples in the series.

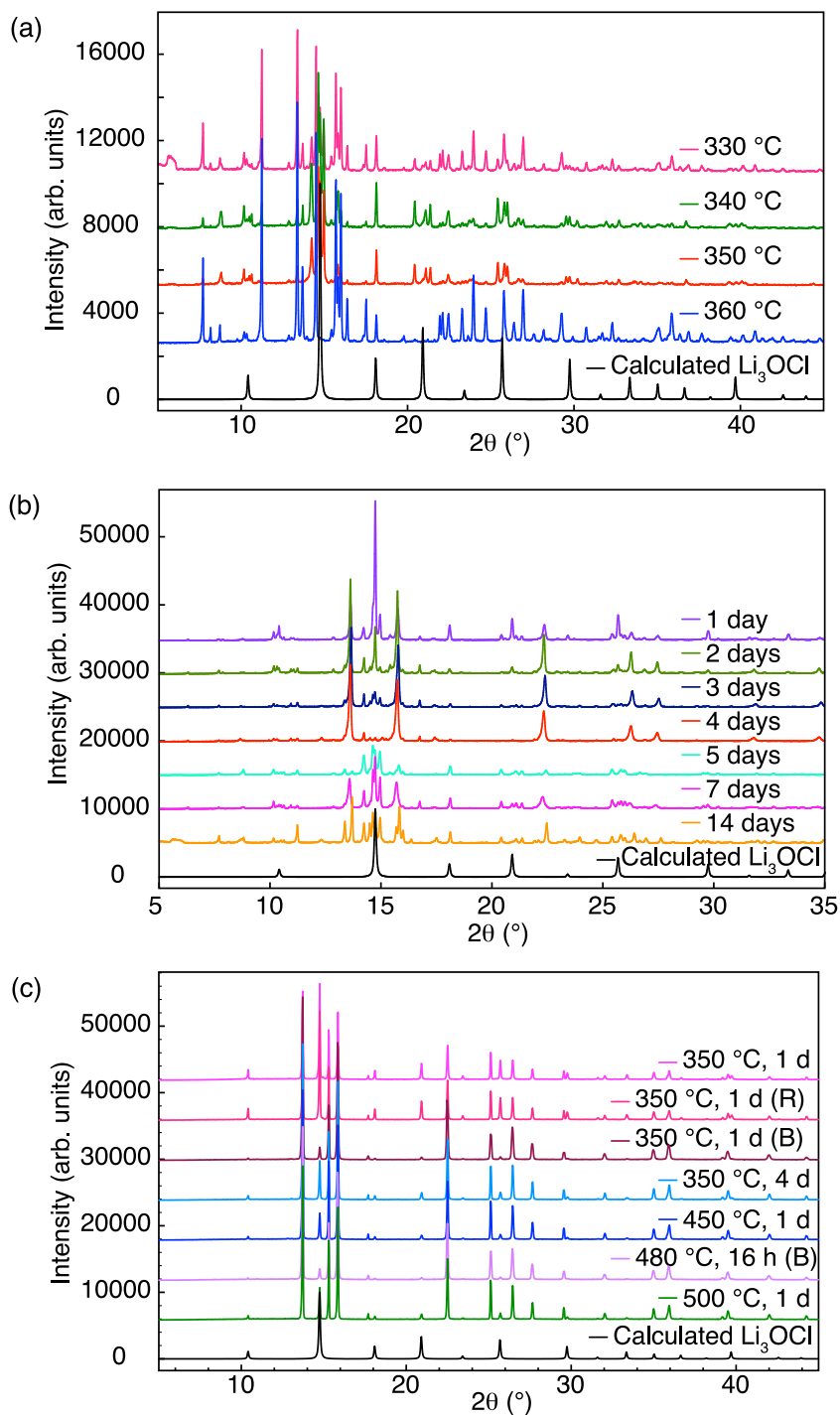


Figure S1. Laboratory X-ray diffraction patterns obtained during the synthesis of Li_3OCl . All samples in (a) and (b) were synthesised via heating under vacuum using a conventional Schlenk line. In (a), the reaction time was fixed at 100 h and the reaction temperature was varied from 330–360 °C. In (b), the reaction temperature was fixed at 360 °C and the reaction time was varied between 24 h and 14 d. In (c), conventional solid-state reactions were completed inside an argon-filled glovebox. Reactions denoted by (R) indicate an intermediate regrinding was used and those marked with a (B) indicate that ball milling was used.

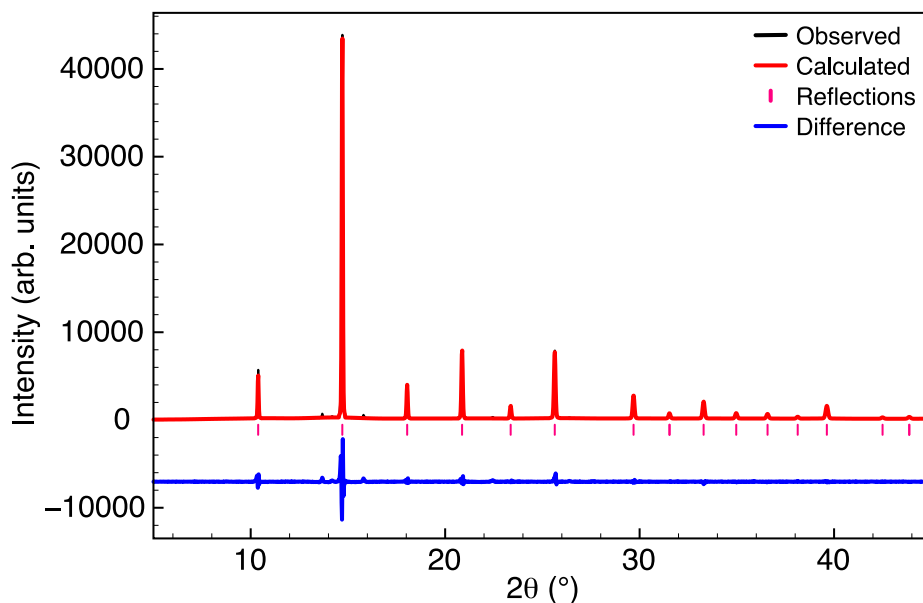


Figure S2. Rietveld refinement for the cubic phase of Li_2OHCl using laboratory X-ray diffraction data and the $Pm\text{-}3m$ structural model.³ The diffraction data was acquired at 50 °C. $\chi^2 = 8.5$, $wR_p = 15.6\%$ and $R_p = 10.3\%$. The Rietveld refinement was completed using the General Structure Analysis System software package.⁴

Table S1. Structural parameters for the cubic phase of Li_2OHCl obtained from Rietveld refinement of laboratory X-ray diffraction data acquired at 50 °C using isotropic thermal factors. Space group $Pm\text{-}3m$, $a = 3.913(1) \text{ \AA}$ and $V = 59.915(4) \text{ \AA}^3$. $\chi^2 = 8.5$, $wR_p = 15.6\%$ and $R_p = 10.3\%$.

Atom	x	y	z	$U(\text{iso}) \times 100/\text{\AA}^2$
Li	0.50	0.50	0.00	5.7(3)
O	0.50	0.50	0.50	2.2(1)
Cl	0.00	0.00	0.00	2.4(1)

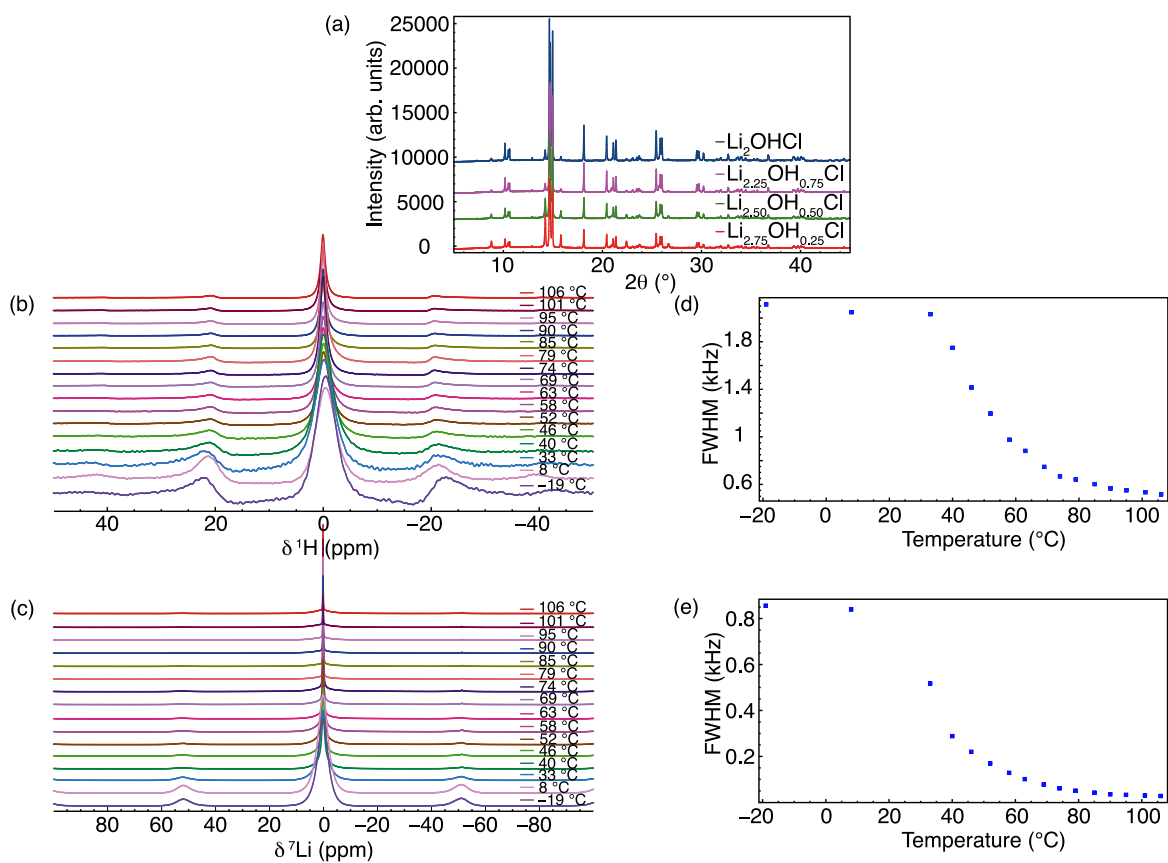


Figure S3. X-ray diffraction patterns obtained for the series $\text{Li}_{3-x}\text{OH}_x\text{Cl}$, where $x = 0.25, 0.5, 0.75$ and 1 . Variable-temperature (b) ^1H and (c) ^7Li MAS NMR spectra obtained for $\text{Li}_{2.75}\text{OH}_{0.25}\text{Cl}$. The corresponding variation in FWHM of ^1H and ^7Li for $\text{Li}_{2.75}\text{OH}_{0.25}\text{Cl}$ are shown in (d) and (e), respectively. All spectra were acquired using a MAS rate of 10 kHz.

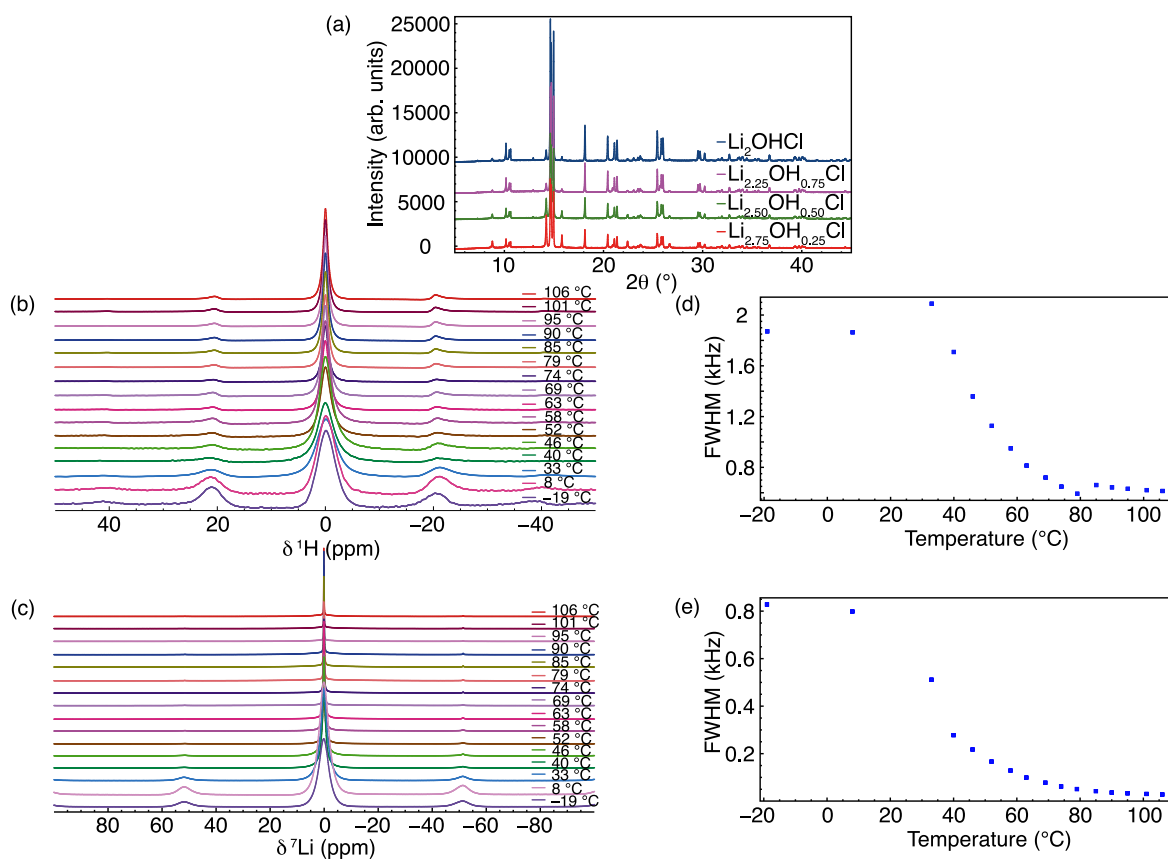


Figure S4. X-ray diffraction patterns obtained for the series $\text{Li}_{3-x}\text{OH}_x\text{Cl}$, where $x = 0.25, 0.5, 0.75$ and 1 . Variable-temperature (b) ^1H and (c) ^7Li MAS NMR spectra obtained for $\text{Li}_{2.25}\text{OH}_{0.75}\text{Cl}$. The corresponding variation in FWHM of ^1H and ^7Li for $\text{Li}_{2.25}\text{OH}_{0.75}\text{Cl}$ are shown in (d) and (e), respectively. All spectra were acquired using a MAS rate of 10 kHz.

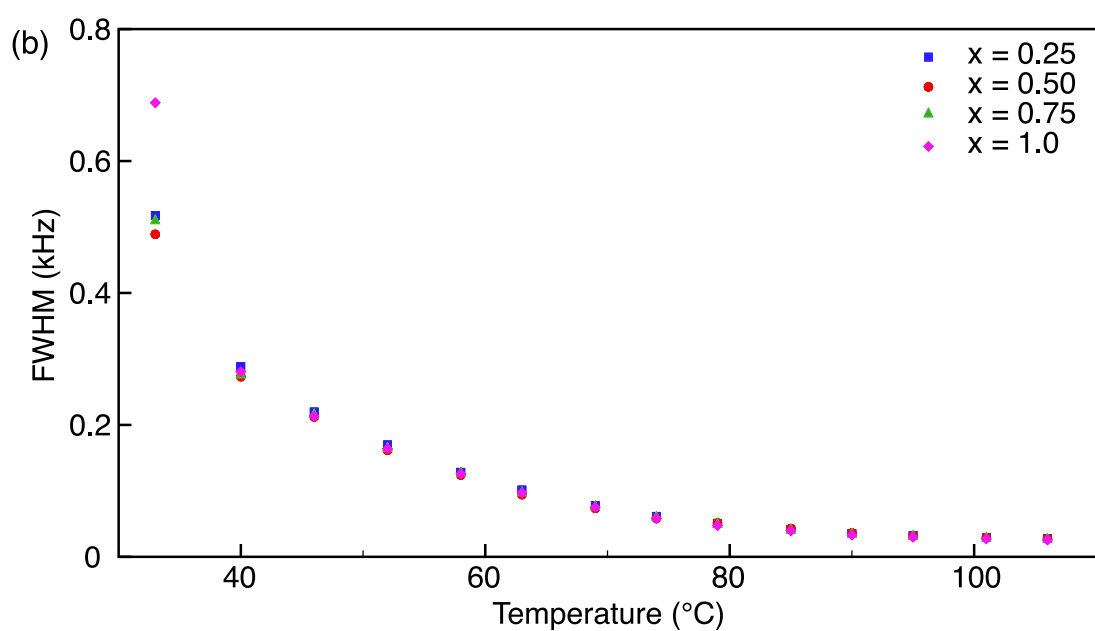
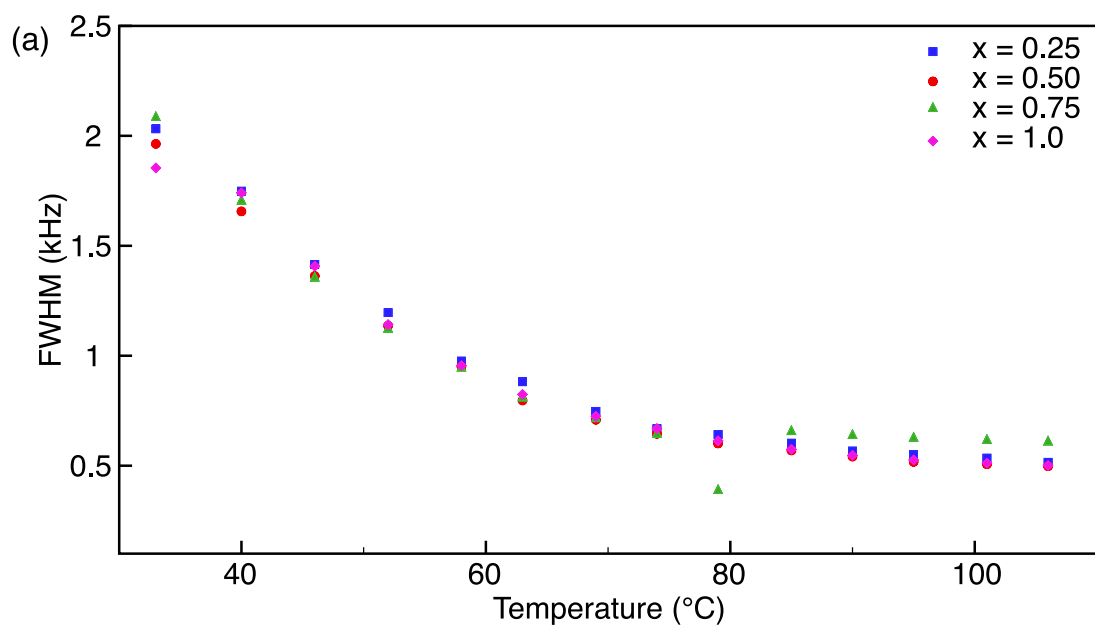


Figure S5. Comparison of the variation in FWHM of (a) ^1H and (b) ^7Li as a function of composition for the series $\text{Li}_{3-x}\text{OH}_x\text{Cl}$, where $x = 0.25, 0.5, 0.75$ and 1 .

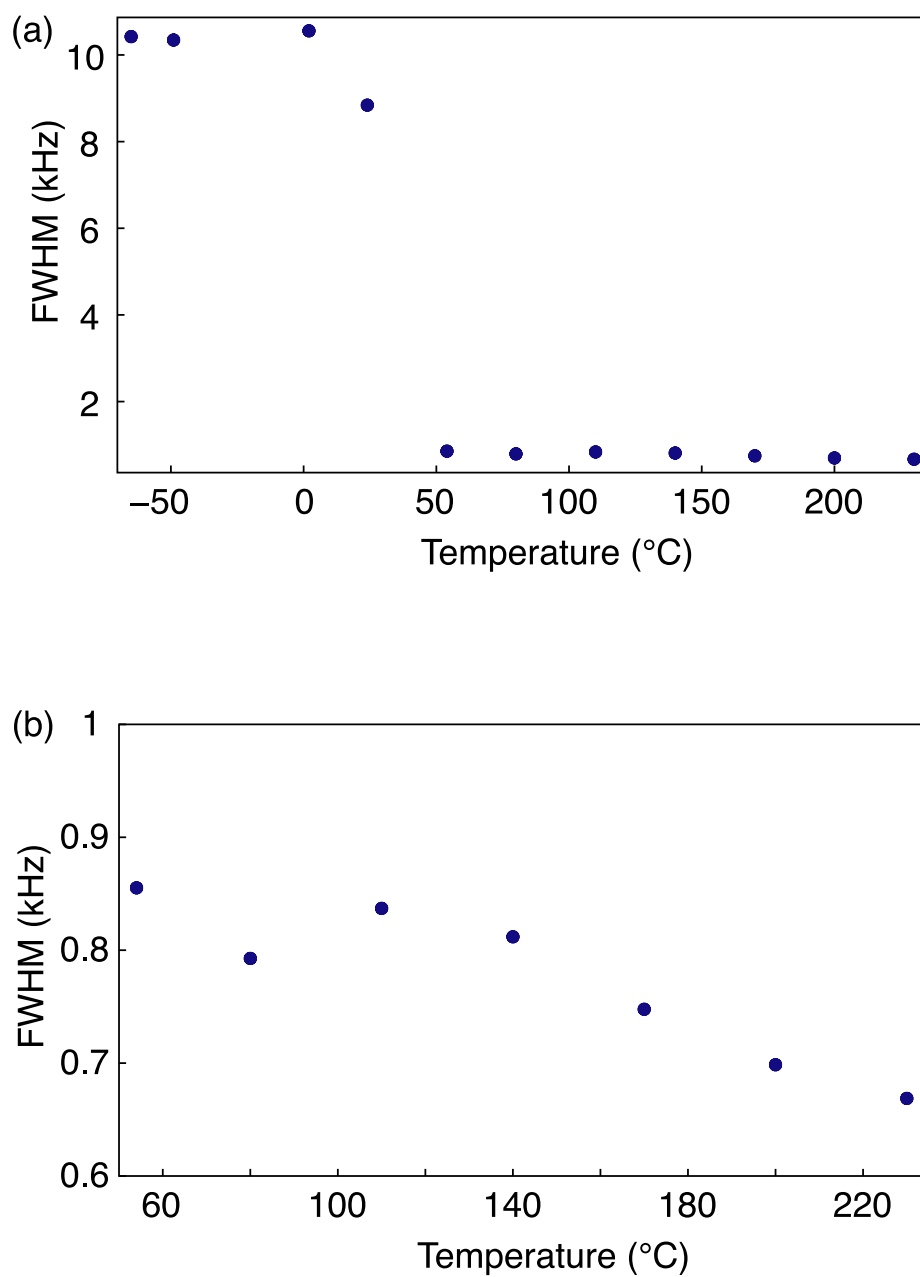


Figure S6. (a) Variation in the ^7Li FWHM for Li_2OHCl obtained from the variable-temperature static ^7Li NMR data shown in Figure 7 in the main manuscript. For clarity, an expansion of the data obtained between 54 and 230 $^{\circ}\text{C}$ is shown in (b).

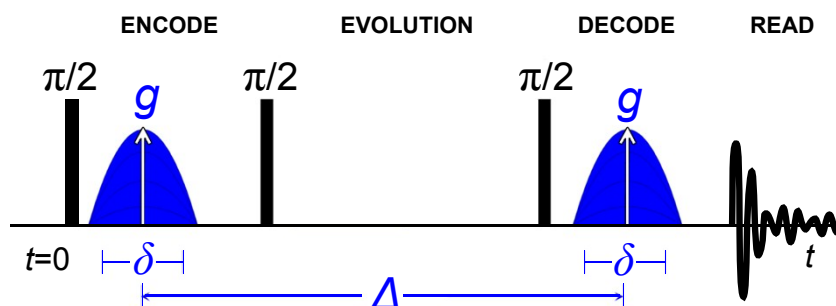
Pulsed-field gradient (PFG) NMR spectroscopy

PFG-NMR spectroscopy is a technique by which ^1H and ^7Li diffusion coefficients, D_{H} and D_{Li} , can be measured. The diffusion coefficient can be extracted from the NMR echo intensity as a function of the magnetic field gradient using the Stejskal and Tanner equation, given by

$$S(g, \delta, \Delta) = \frac{I}{I_0} = \exp \left(- (\gamma \delta g)^2 D \left(\frac{\Delta - \delta}{3} \right) \right) = \exp (- b D), \quad (1)$$

where I is the measured intensity, I_0 is the intensity at the lowest gradient strength, γ is the ^7Li gyromagnetic ratio ($2\pi \cdot 1655 \text{ Hz/G}$), δ the effective gradient length (here, 5 ms), g the gradient strength (here between 0 and 1800 G/cm), Δ is the diffusion time between the two gradient pulses (here, 100, 175 or 250 ms) and D is the apparent diffusion coefficient of the observed nucleus.⁵

PFG-NMR spectra were acquired for Li_2OHCl using the stimulated echo pulse sequence shown in Scheme S1. Spectra were acquired at elevated temperatures of 373 K after an equilibration time of at least 1 hour. It is noted that at higher temperatures the values of T_1 decreased substantially, leading to very fast acquisition times and longer gradient pulses due to longer T_2 relaxation times.



Scheme S1. Stimulated echo diffusion pulse sequence typically used for the acquisition of PFG-NMR spectra of solid materials when $T_1 \gg T_2$. After the first gradient pulse, a z-storage delay is introduced, which leads to longer observation times, as the magnetisation is not affected by T_2 relaxation in this period.

⁷Li PFG-NMR Measurements

To determine the diffusion coefficient of Li₂OHCl, the ⁷Li echo signal intensity was obtained as a function of the magnetic field gradient, g . The signal shows a decrease in intensity, I , with increasing gradient strength, indicative of Li mobility and diffusion. Analysis of the data indicates a $D_{\text{Li}} \approx 6 \times 10^{-13}$ m²/s at 373 K. Hence, ⁷Li PFG-NMR measurements confirm long range Li diffusion at 373 K, in good agreement with the ⁷Li MAS NMR data.

Plotting the normalised natural logarithm of the intensity I against b (a summary of constants and parameters detailed in equation 1) the diffusion coefficient, D_{Li} , can be obtained from a linear fit of equation 1 (Figure S8). The diffusion coefficients extracted are summarised in Table S2. In restricted systems (e.g., pores or finite sized particles) the diffusion coefficient often shows a decrease at longer diffusion times. This appears to be the case for Li₂OHCl at 373 K (Figure S9). However, further analysis is needed to determine precisely what factors are affecting Li diffusion within this particular system, which is outside of the current study.

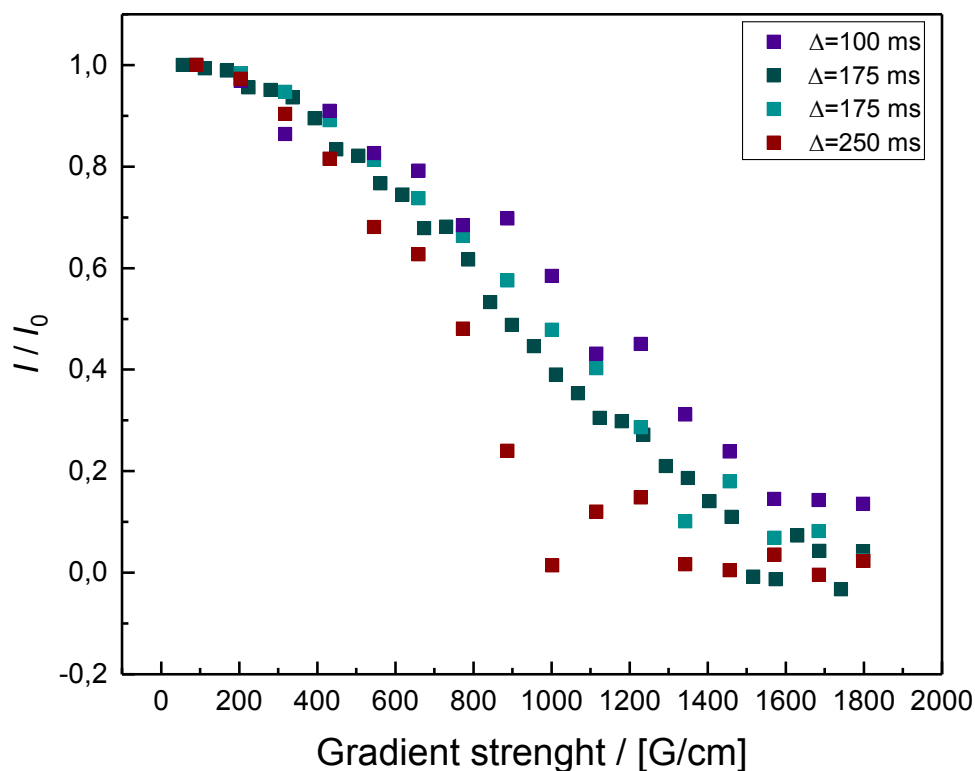


Figure S7. The decaying ⁷Li signal intensity, I/I_0 , plotted against the applied gradient strength for Li₂OHCl at 373 K for a range of diffusion times, Δ . The data shows faster decay at longer diffusion times, as expected.

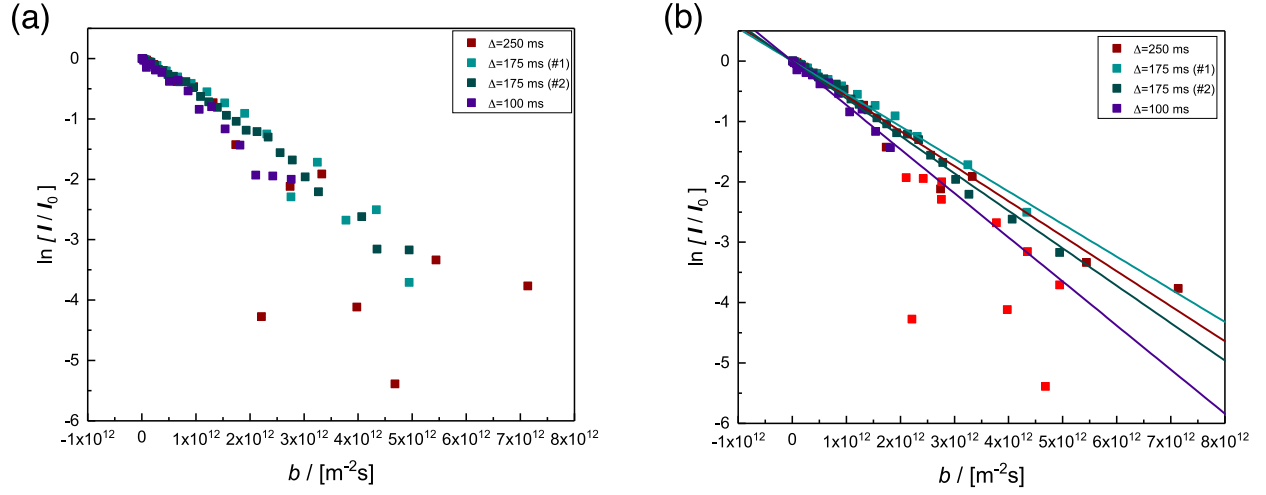


Figure S8. (a) Natural logarithm of the intensity I/I_0 plotted against b (a summary of the constants and parameters detailed in equation 1) and (b) the fitted data points for Li_2OHCl at 373 K. The data points in red were considered as outliers and have not been included in the fits.

Table S2. Summary of the Li diffusion coefficients, D_{Li} , obtained for Li_2OHCl at 373 K, extracted from the data shown in Figure S8(b).

Δ/ms	$D_{\text{Li}} / [\text{m}^2/\text{s}]$
250	$5.8 \cdot 10^{-13} \pm 2.4 \cdot 10^{-14}$
175 (#1)	$5.4 \cdot 10^{-13} \pm 1.2 \cdot 10^{-14}$
175* (#2)	$6.2 \cdot 10^{-13} \pm 7.3 \cdot 10^{-15}$
100	$7.3 \cdot 10^{-13} \pm 2.4 \cdot 10^{-14}$

*#2 used 32 different gradient strengths instead of 16

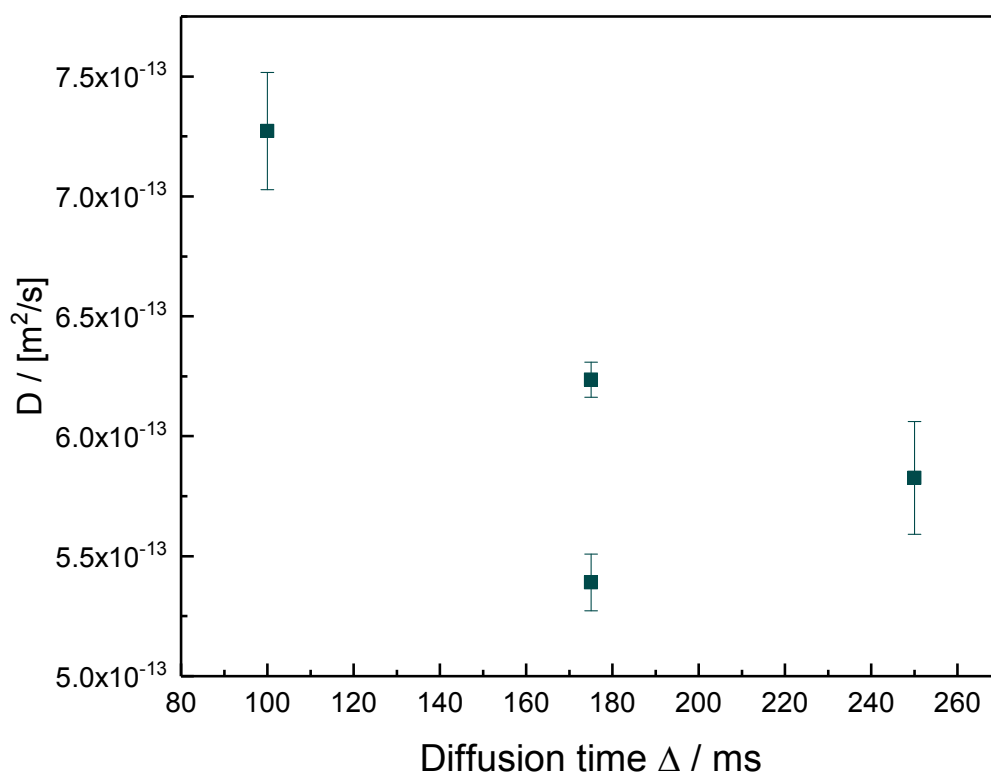


Figure S9. Trend in Li diffusion coefficients for Li_2OHCl at 373 K as a function of diffusion time.

^1H PFG-NMR Measurements

^1H diffusion measurements were also completed for Li_2OHCl using PFG-NMR. ^1H PFG-NMR experiments were completed using the stimulated diffusion pulse sequence above on a Bruker AV 300 spectrometer equipped with a PFG Bruker probe (30 T/m). However, no evidence of proton diffusion was observed, in good agreement with the ^1H and ^2H MAS NMR data presented. In the ^1H PFG-NMR measurements, no signal attenuation as a function of the gradient strength was observed (Figure S10). Typically (as in the case of the ^7Li PFG-NMR measurements above), the signal intensity is plotted as a function of the gradient strength. However, in this case it is not possible, owing to significant dephasing between the first and last spectrum of the two-dimensional dataset acquired. Hence, the first and last raw datasets of the two-dimensional spectra were extracted to demonstrate that the magnitude of the signal remains the same both with and without gradient pulses. Hence, as no signal attenuation is observed as a function of the gradient strength there is no evidence for proton diffusion. This is also confirmed by the lack of diffusion coefficient obtained, D_{H} , which, at both room temperature and 373 K, is *well below* $1 \times 10^{-12} \text{ m}^2/\text{s}$ (**the lowest measurable value within the TopSpin software**). Hence, all of the data presented confirms limited proton mobility within Li_2OHCl .

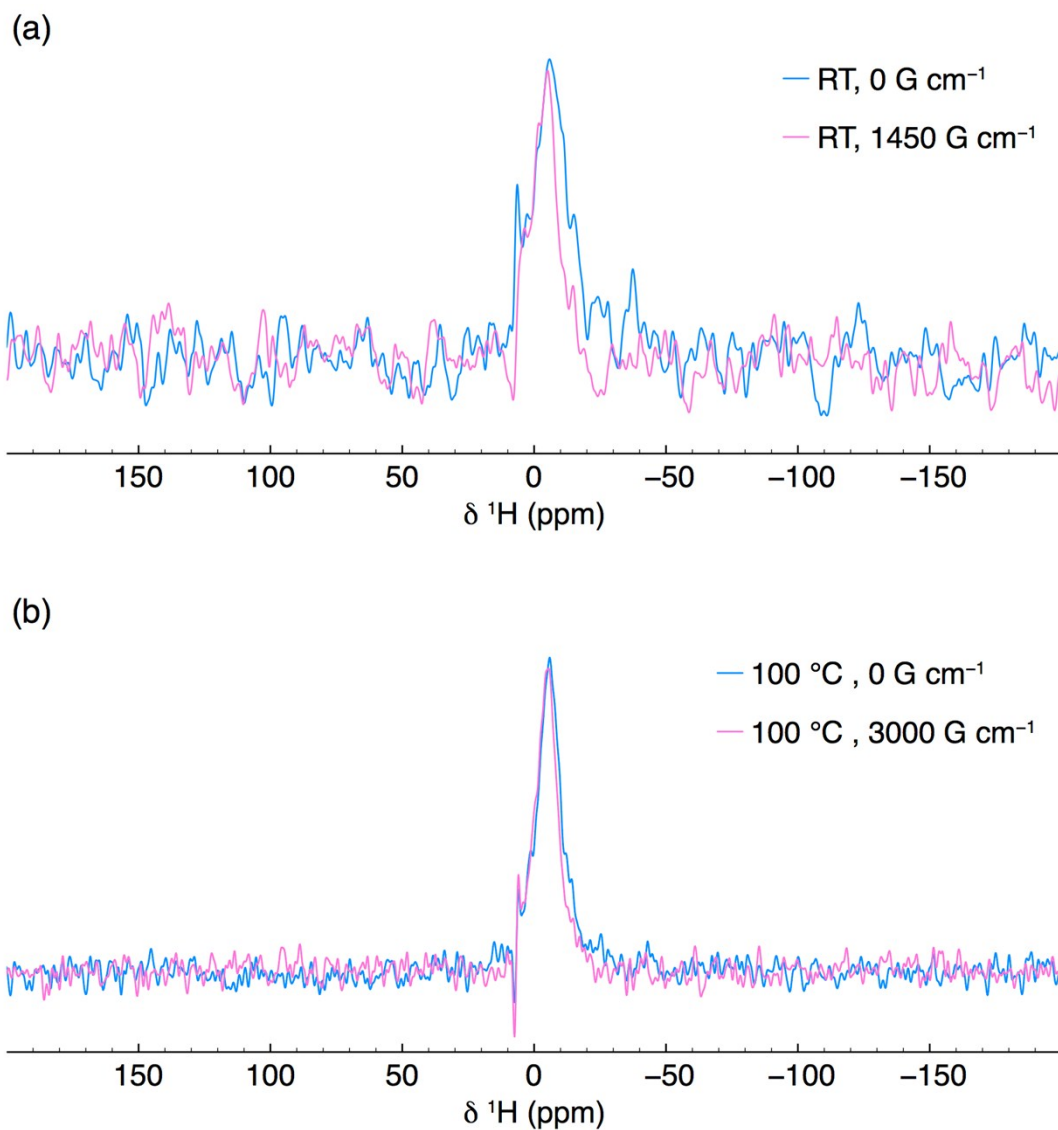


Figure S10. ^1H PFG-NMR spectra obtained at (a) room temperature and (b) 373 K. In both cases, spectra were extracted from two-dimensional datasets and represent the first (0 G cm⁻¹) and last (1450 or 3000 G cm⁻¹) spectra obtained in the dataset. In both cases, no change in intensity is observed, indicating no ^1H diffusion.

In NMR spectroscopy, ^2H ($I = 1$) is the most commonly exploited quadrupolar nucleus for studying molecular dynamics and motion in solids. However, its very low natural abundance (0.012%) makes isotopic enrichment necessary, which can be quite challenging. The most common method for extracting dynamic information using ^2H NMR is to record the powder pattern for a stationary sample using a spin-echo experiment. In the absence of motion, a well-defined Pake doublet with a quadrupolar splitting is obtained. In the presence of motion, the lineshape will become distorted, which will be influenced by the precise geometry and rate of the motion observed. In some cases, it can be challenging to derive the underlying types of motion from static ^2H NMR experiments. MAS NMR experiments can also be used, where the manifold of spinning sidebands outlines the shape of the static powder pattern.

The room temperature XRD pattern obtained for the deuterated sample of Li_2OHCl , Li_2ODCl , is shown below, which confirms that the deuteration process does not affect the product formed. The presence of static OH^-/OD^- groups at low temperatures (Figures 8 and S11) is in good agreement with both the ^1H MAS NMR data (Figure 1) and the tetragonal ground state structure proposed from our AIMD calculations, in which all of the OH^-/OD^- groups are aligned along the a direction (Figure 2). The ^2H MAS NMR spectrum acquired at 63 °C (Figure 8) exhibits an obvious reduction in signal-to-noise, likely indicative of a change in the relaxation properties of the system, most notably a change in the spin-spin (T_2) relaxation.

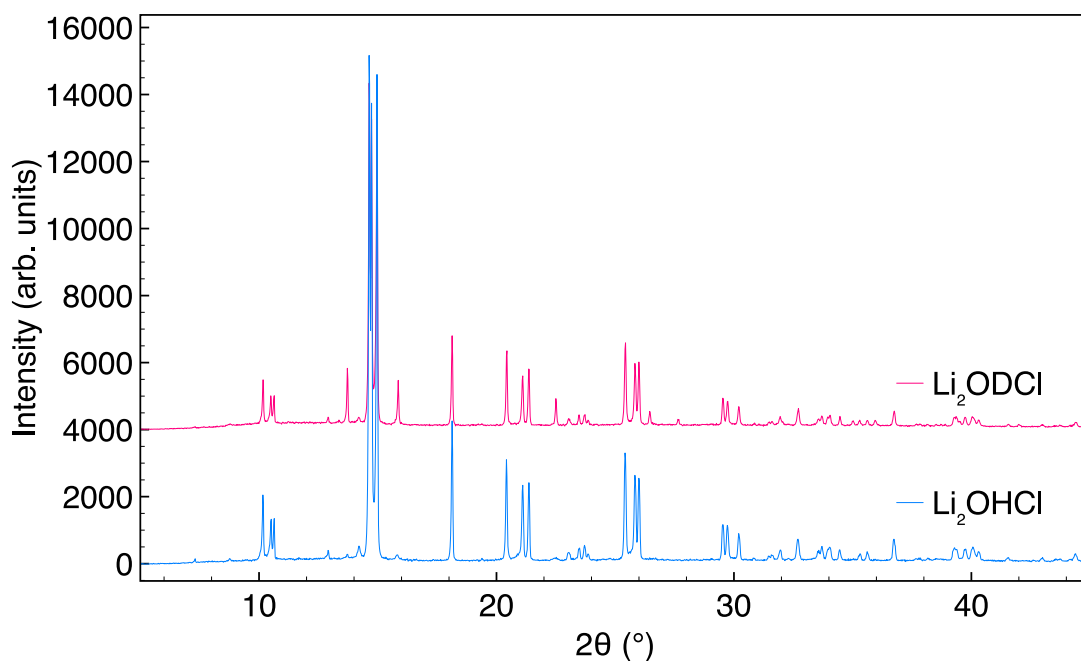


Figure S11. X-ray diffraction patterns obtained for Li_2OHCl and Li_2ODCl at room temperature.

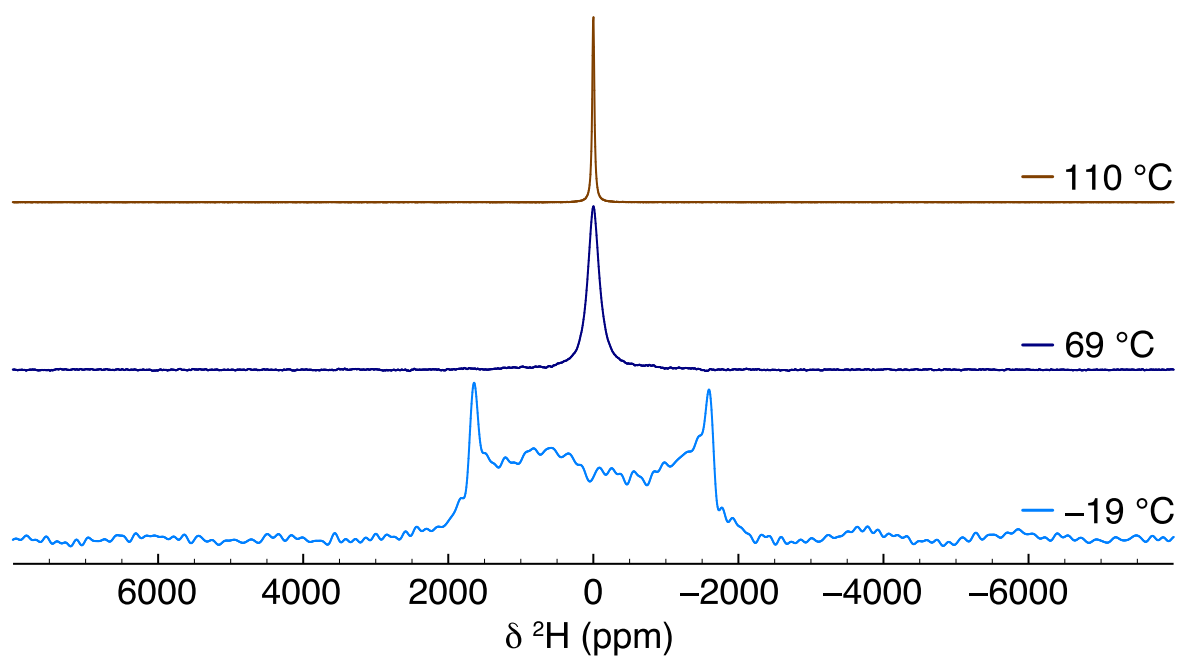


Figure S12. Variable-temperature static ^2H NMR spectra acquired for Li_2ODCl at -19 , 69 and 110 $^\circ\text{C}$.

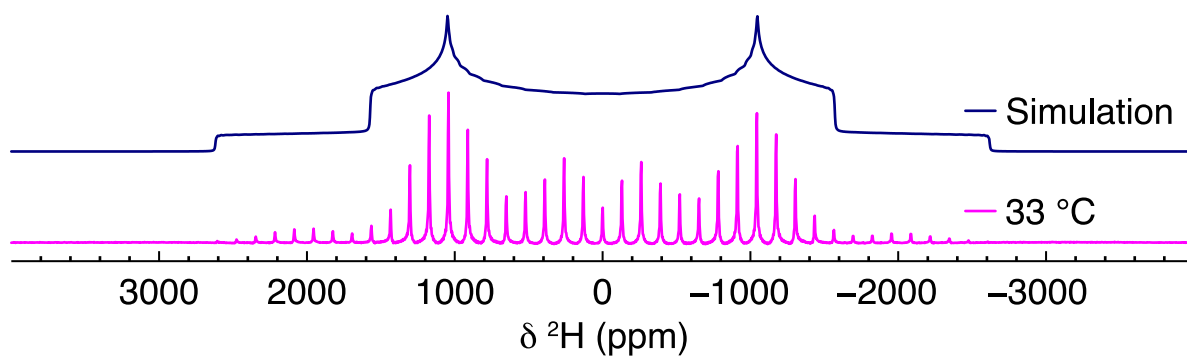


Figure S13. ^2H MAS NMR data obtained for Li_2ODCl at 33 $^\circ\text{C}$. The spectrum was simulated to obtain the corresponding quadrupolar parameters, $C_Q = 259(1)$ kHz and $\eta_Q = 0.0(1)$.

References

- 1 D. G. Cory, W. M. Ritchey, *J. Magn. Reson.*, 1988, **80**, 128.
- 2 B. M. Fung, A. K. Khitrin, K. Ermolaev, *J. Magn. Reson.*, 2000, **142**, 97.
- 3 P. Hartwig, A. Rabenau, W. Weppner, *J. Less Common Met.* 1981, **78**, 227.
- 4 A. C. Larson, R. B. von Dreele, Los Alamos National Laboratory, Report No. LA-UR-86-748, 1987.
- 5 E. O. Stejskal, J. E. Tanner, *J. Chem. Phys.* 1965, **42**, 288.